Magnetic order and ice rules in the multiferroic spinel FeV$_2$O$_4$

G. J. MacDougall,[1,*] V. O. Garlea,[1] A. A. Aczel,[1] H. D. Zhou,[2,3] and S. E. Nagler[1,4]

[1]*Quantum Condensed Matter Division, Oak Ridge National Laboratory, Oak Ridge, Tennessee 37831, USA*
[2]*Department of Physics and Astronomy, University of Tennessee, Knoxville, Tennessee 37996, USA*
[3]*National High Magnetic Field Laboratory, Tallahassee, Florida 32310, USA*
[4]*CIRE, University of Tennessee, Knoxville, Tennessee 37996, USA*

We present a neutron-diffraction study of FeV$_2$O$_4$, which is rare in exhibiting spin and orbital degrees of freedom on both cation sublattices of the spinel structure. Our data confirm the existence of three structural phase transitions previously identified with x-ray powder diffraction and reveal that the lower two transitions are associated with sequential collinear and canted ferrimagnetic transitions involving both cation sites. Through consideration of local crystal and spin symmetry, we further conclude that Fe^{2+} cations are ferro-orbitally ordered below 135 K and V^{3+} orbitals order at 60 K, in accordance with predictions for vanadium spinels with large trigonal distortions and strong spin-orbit coupling. Intriguingly, the direction of ordered vanadium spins at low temperature obey "ice rules" more commonly associated with the frustrated rare-earth pyrochlore systems.

PACS number(s): 75.25.Dk, 61.05.F−, 75.47.Lx, 75.85.+t

Magnetic insulators with orbital degrees of freedom are of great interest to both the condensed-matter and applied physics communities. Transition-metal spinels are a particular example where orbital degeneracy and the concomitant orbital ordering have been shown to profoundly affect both the crystal structure and magnetic exchange interactions.[1,2] In recent years, the material FeV$_2$O$_4$ has emerged as an important model system to explore this physics. A rare example of a spinel with two orbitally active cation sites, FeV$_2$O$_4$ is a multiferroic, containing both ferroelectric[3] and ferrimagnetic moments[3–6] at low temperatures. Moreover, separate experiments have demonstrated that the applied magnetic fields can both suppress the ferroelectric moments[6] and induce structural detwinning.[6] Previous x-ray diffraction measurements[6] mapped out a sequence of structural phase transitions; however, despite the obvious importance of magnetoelastic and magnetoelectric coupling, magnetic structures have remained unknown. In this Rapid Communication, we present new neutron-scattering data definitively solving the magnetic structures as a function of temperature. The results establish that FeV$_2$O$_4$ contains unexpected and very interesting parallels to the well-known spin-ice problem of frustrated magnetism,[7] realized at low temperatures in selected rare-earth-containing pyrochlore materials.

The spinel vanadates, AV$_2$O$_4$, with divalent A-site cations have been central to the study of orbital order and the role of orbital degrees of freedom in geometrically frustrated antiferromagnets. In these systems, the pyrochlore sublattice of the spinel structure is occupied by V^{3+} ($3d^2$) cations in an octahedral oxygen environment, giving spin $S = 1$ and an orbital triplet degree of freedom. Materials such as ZnV$_2$O$_4$,[8–10] CdV$_2$O$_4$,[11] and MgV$_2$O$_4$,[12–14] where the A site is magnetically neutral, are typified by two transitions: an orbital ordering transition which lowers crystal symmetry at an upper temperature, followed by a second magnetic transition to a state with a complex pattern of ordered spins. In MnV$_2$O$_4$, with spin-only Mn^{2+} on the A site, the system first orders magnetically to a collinear spin state involving both cation sites, only to develop a noncollinear structure below

a second transition at a lower temperature.[15–18] Despite being electronically and structurally similar at high temperatures, the low-temperature properties of these materials are strikingly different, as the relative importance of spin-orbit coupling and tetragonal and trigonal crystal fields vary in different systems. In each of these materials, debate continues and centers on understanding the nature of the orbital order inferred from measured crystal symmetry and magnetic structure.[19–25] A largely separate line of research has concentrated on the role of orbitals on the A-site sublattice, for example, in FeCr$_2$O$_4$ (Refs. [26–29]) or FeSc$_2$S$_4$;[30,31] however, very few materials have been identified with orbitally active ions on *both* cation sites of the spinel structure.

In this regard, FeV$_2$O$_4$ is an extraordinary material. In addition to V^{3+} on the pyrochlore sublattice, this system contains tetrahedrally coordinated Fe^{2+} ($3d^6$) cations on the A site of the spinel structure with high-spin $S = 2$ and twofold orbital degeneracy. As might be expected, further interactions result in additional complex and interesting behavior. Specific-heat measurements have revealed three phase transitions in this material with $T_c = 138$, 111, and 56 K.[3] Powder x-ray scattering[6] has associated these temperatures with a cascade of structural transitions, from cubic to high-temperature tetragonal (HTT) to face-centered orthorhombic (FCO) to low-temperature tetragonal (LTT) with decreasing temperature. Both Mössbauer[5] and magnetization[3,6] measurements indicate that at least one of these transitions (HTT → FCO) additionally involves the ordering of magnetic degrees of freedom. A fourth structural phase transition to low-temperature orthorhombic (LTO) symmetry has been reported in one single crystalline study,[6] and at least one ac-susceptibility study has identified a glasslike transition at 85 K.[32] Despite these advances and the implied coupling of electric, lattice, and magnetic degrees of freedom, very little is known about the local spin and orbital structure in the distinct phases of FeV$_2$O$_4$.

In this Rapid Communication, we present results of a neutron powder diffraction (NPD) study of FeV$_2$O$_4$ at temperatures below 200 K. We confirm the cubic-HTT-FCO-LTT sequence of structural phase transitions reported by powder
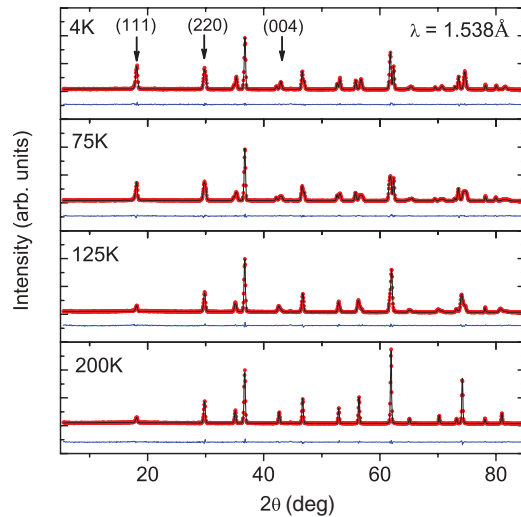
FIG. 1. (Color online) Plots of raw NPD data (circles) measured at $T = 200$, 125, 75, and 4 K for $2\theta \leqslant 85°$. Solid lines are results of Rietveld refinements described in the main text. Differences between observed and calculated intensities are shown directly below the respective patterns. See the main text and Fig. 2 for more detail.
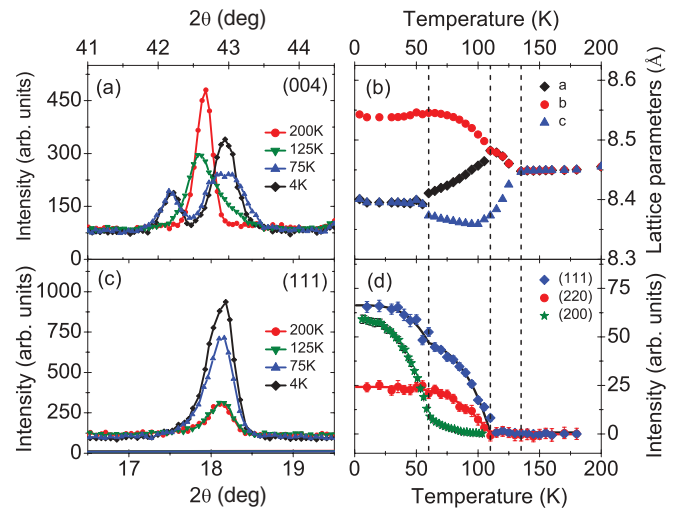

FIG. 2. (Color online) (a) An expanded view of the NPD data around the cubic (004) Bragg position for each of the patterns in Fig. 1. (b) Plot of the cubic lattice parameters extracted from NPD data. (c) An expanded view around the cubic (111) Bragg position for the same temperatures as (a). (d) A comparison of the temperature evolution of NPD (111) and (220) Bragg peak intensities above their values at 180 K. Overlaid is the scaled intensity of the (200) Bragg peak, as measured in a single-crystal sample.

x-ray scattering[6] but see no evidence for the purported fourth transition to a low-temperature orthorhombic phase.[6] We discuss the evolution of the crystal-field environment of V^{3+} cations and in particular present evidence for a large trigonal distortion of the octahedral oxygen cage about these sites. We additionally report the existence of two separate magnetic ordering transitions: a collinear spin ordering coincident with the HTT-FCO transition and a tilting of V^{3+} moments to point along the $\langle 111 \rangle$ crystal directions when symmetry changes from FCO to LTT. We discuss the implications of the current observations for the orbital order and in particular argue that this material is well described by models which assume large trigonal distortion and strong spin-orbit coupling.

Polycrystalline samples of FeV_2O_4 were prepared by solid-state reaction, and NPD measurements were performed using the HB2A diffractometer at the High Flux Isotope Reactor (HFIR).[33] Further elastic neutron-scattering data were taken on a crystal grown via the float zone method using the CG-4C Cold Neutron Triple-Axis Spectrometer of HFIR. Details about sample preparation and experimental method can be found in the Supplemental Material, along with characterization data on both powder and single-crystal samples.[34]

The results of our high-resolution neutron-diffraction measurements at 200, 125, 75, and 4 K are shown in Fig. 1 for $2\theta \leqslant 85°$. The highest-temperature data confirm the spinel structure at these temperatures and the near phase purity. Refinement implies that a fraction of the vanadium sites is occupied by iron cations, giving the chemical formula $Fe[Fe_{0.058}V_{0.942}]_2O_4$. This is similar to other samples in the literature.[3,6] There is also a small temperature-independent impurity phase, possibly associated with an oxide of vanadium. The temperatures of remaining high-resolution patterns were chosen to be well within each of the five phases identified by Katsufuji *et al.* with single-crystal x-ray diffraction.[6] Contrary to those results, however, no discernible difference was seen

between the patterns at 50 and 4 K, and so only the 4 K pattern is plotted here. The four unique patterns were well described by the space groups $Fd\bar{3}m$, $I4_1/amd$, $Fddd$, and $I4_1/amd$ with decreasing temperature, consistent with previous analysis and reflecting the cubic-HTT-FCO-LTT sequence of structural phase transitions.[6] Patterns to $2\theta = 154°$ and full refinement information are given as Supplemental Material, along with a more in-depth discussion of the absent LTT-LTO phase transition.[34]

The sequence of observed structural transitions is illustrated more clearly in Figs. 2(a) and 2(b). Figure 2(a) shows the successive splittings and recombination of the cubic (004) peak for each of the four patterns. Figure 2(b) shows a plot of the lattice parameters extracted from lower-resolution NPD data assuming the crystal symmetries determined above. (For the sake of comparison, all lattice parameters plotted here are those for the cubic unit cell.) Transition temperatures are identified as 135, 110, and 60 K, within an uncertainty of 5 K. These estimates are similar to the values inferred from heat capacity in recent measurements of powders by Zhang *et al.*,[3] as well as our own single-crystal data (see Supplemental Material[34]).

Figures 2(c) and 2(d) demonstrate the neutron-scattering intensity of the cubic (111) peak as a function of temperature. Contrary to what is expected from structural considerations alone, NPD reveals a significant increase in this peak below the HTT → FCO transition and again below the FCO → LTT transition. At both temperatures, an increase in net moment has been noted in bulk magnetization data.[3,6] For comparison, we also show in Fig. 2(d) the temperature evolution of the (220) peak from NPD and the (much weaker) (200) peak from single-crystal elastic scattering. The (220) peak carries only information about the iron sublattice, and its temperature dependence reflects only the 110 K transition. Conversely, the intensity of the (200) peak is zero at high temperature
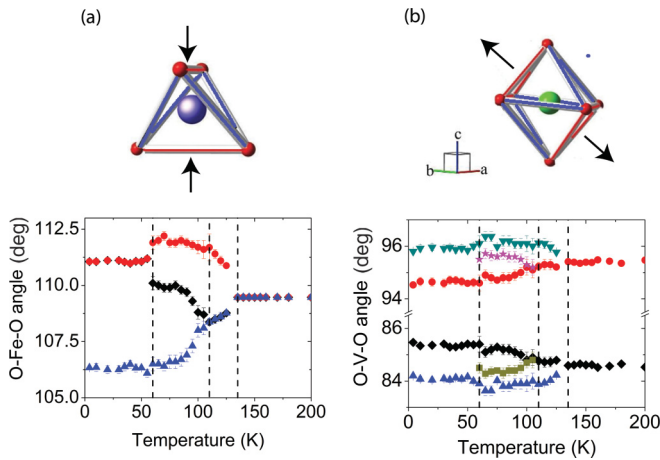
FIG. 3. (Color online) Plots vs temperature of the interior O-M-O angles $[M \in (Fe^{2+}, V^{3+})]$ of the (a) FeO_4 tetrahedra and (b) VO_6 octahedra, shown schematically at the top. In pictures, bonds of equal length are shown with equivalent coloring. Arrows denote the largest distortion of each polyhedron: a compression of the FeO_4 tetrahedron at 135 K along [001] and a trigonal distortion of the VO_6 octahedron along the $\langle 111 \rangle$ directions that exists at all temperatures.

and grows below the transition at 60 K. These observations are consistent with our Rietveld refinements, which associate the two lowest phase transitions with the onset of collinear and canted ferrimagnetism, as discussed in more detail below.

To gain insight about the crystal-field environment at the Fe^{2+} and V^{3+} sites, we further plot in Fig. 3 the O-cation-O angles as a function of temperature for the FeO_4 tetrahedra and VO_6 octahedra, respectively. In the high-temperature cubic $(Fd\bar{3}m)$ phase, the interior angles of the FeO_4 tetrahedra [Fig. 3(a)] are sixfold degenerate with a value of $109.4°$. This reflects the fact that the tetrahedra are regular, and thus the orbital ground state of Fe^{2+} is twofold degenerate. At the 135 K transition, this degeneracy is lifted by a uniform compression in the cubic (001) direction, lessening four of the six O-Fe-O angles and lowering the energy of the single-electron d_{z^2} orbital relative to the $d_{x^2-y^2}$ orbital. As noted previously by Katsufuji *et al.*[6] and Sarkar and Saha-Dasgupta,[35] this behavior can be associated with ferro-orbital order on the Fe^{2+} site. The orthorhombic transition introduces an additional in-plane compression of the tetrahedra, which increases with decreasing temperature until the system locks in to the low-temperature tetragonal structure. Notably, these subsequent transitions affect all Fe^{2+} equivalently and are consistent with ferro-orbital order persisting to the lowest temperatures (though the exact distribution of electron density will evolve upon cooling).

Conversely, in the $Fd\bar{3}m$ phase the VO_6 octahedra display a significant trigonal distortion from cubic symmetry. This is evident in Fig. 3(b), where one can see that at high temperatures the 12 interior angles of the VO_6 octahedra are split into two inequivalent branches of six with values significantly different from $90°$ (expected for regular octahedra). This splitting corresponds to a stretching of the octahedra in alternating $\langle 111 \rangle$ directions along chains in the [110] direction. The distortion can be associated directly with the oxygen
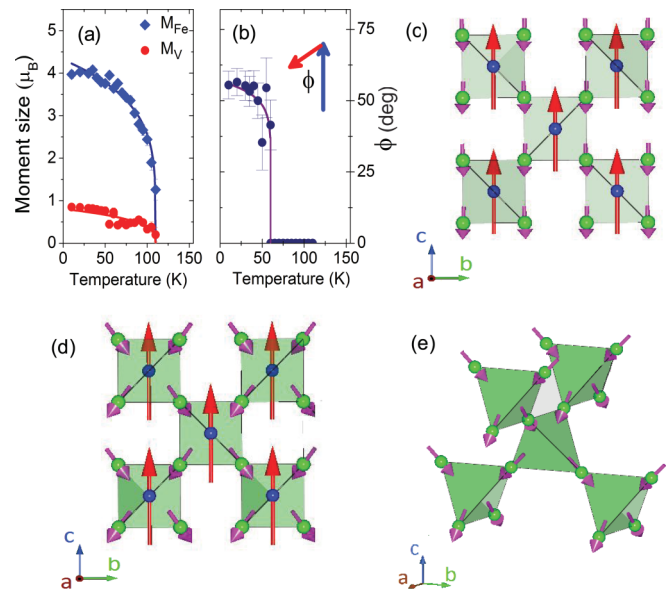

FIG. 4. (Color online) (a) Plot of the ordered moment size on the Fe^{2+} and V^{3+} cation sites and (b) the angle between the V^{3+} moments and the axis defined by Fe^{2+} moments. (c) A sketch of the collinear ferrimagnetic state in the FCO phase, as seen along the cubic (001) direction and (d) a similar sketch of the canted state seen in the LTT phase. Details about the ordering patterns are given in the main text. (e) A view of V^{3+} moments in a low-temperature ordered state clearly demonstrating the two-in–two-out spin structure on the pyrochlore sublattice.

position parameter within the $Fd\bar{3}m$ space group. The angular separation at high temperatures $(10.7°)$ is comparable to what is inferred from the structures of MnV_2O_4 $(12.9°)$ and $MgV_2O_4(8.7°)$, where the importance of trigonal distortion has already been acknowledged.[14,24,25] Katsufuji *et al.* previously noted a tetragonal compression of the VO_6 octahedra at the 135 K transition.[6] This is observable in Fig. 3(b) as well. Notably, however, the trigonal splitting of the O-V-O angles in the cubic state is nearly ten times larger than the perturbations at lower temperatures. (Note the break in the vertical axis.) Thus our data imply that the trigonal distortion is the dominant noncubic term in the crystal-field environment of V^{3+}.

Information about the determined magnetic structure is displayed in Fig. 4. As hypothesized previously in analogy to other spinel systems,[3,6] the HTT → FCO structural phase transition coincides with the onset of collinear ferrimagnetism, wherein Fe^{2+} moments align ferromagnetically along the longest orthorhombic axis and V^{3+} moments align antiparallel. This is the ordered state favored by antiferromagnetic superexchange between the Fe^{2+} and V^{3+} cations and implies that the transition is driven by such magnetic interactions. The orthorhombic structural transition then likely results from a coupling between cation spins and phonon modes, which strongly affect superexchange paths, similar to what has been suggested by recent optical measurements of $FeCr_2O_4$ and $NiCr_2O_4$.[29] As shown in Fig. 4(a), the ordered moment sizes on both sublattices grow below $T_{N1} = 110$ K, with the vanadium moment perhaps seeing an additional increase at 60 K. The ordered moment sizes at the lowest temperatures are $4.0\mu_B$ and $0.85\mu_B$ on the Fe^{2+} and V^{3+} sites, respectively. Whereas

the number for Fe^{2+} is in line with expectations for an $S = 2$ system, the value for V^{3+} is significantly less than the $2.0\mu_B$ expected for an $S = 1$ cation with quenched orbital angular momentum.

Refinements indicate no tendency for V^{3+} to cant away from the axis defined by the Fe^{2+} moments in the orthorhombic phase, although symmetry would allow such behavior. Nonetheless, it is shown in Fig. 4(b) that the refined angle between the V^{3+} moment and the Fe^{2+} spin axis jumps abruptly from zero to $\sim 55° \pm 4°$ below the FCO-LTT transition at $T_{N2} = 60$ K. This canting transition is illustrated in Figs. 4(c) and 4(d), where we sketch the ordered states above and below T_{N2} as viewed along the cubic (100) direction. The existence of a canting transition is further supported by the single-crystal data in Fig. 2(d), as the intensity of the (200) Bragg peak is proportional to the square of the in-plane vanadium moment in this model. The low-temperature value of $55°$ for the canting differs from the $33°$ inferred recently by Kang *et al.* from NMR data.[36] However, as noted previously,[36] a value of $33°$ cannot be reconciled with the large ferrimagnetic moment observed via magnetization[3] (which implies an angle closer to $60°$). We feel that the neutron-diffraction data provide the more reliable estimate.

The evolution from a collinear to canted ferrimagnetic state is reminiscent of the magnetic behavior of MnV_2O_4, where the canting was accompanied by the gapping of magnetic excitations.[17] Significantly though, we note that the canting angle observed here is smaller than the $65°$ reported for MnV_2O_4[17] and is equal within error to the $54.7°$ between the (001) and (111) directions in a cubic lattice. In addition to the canting angle, the "in-plane" [i.e., $\perp$(001)] spin directions imposed by the $I4_1/amd$ space group are also different from what has been assumed for the ordered state of MnV_2O_4,[17] and in fact refinement suggests the low-temperature phase of FeV_2O_4 is characterized by a "two-in–two-out" structure on the pyrochlore lattice [see Fig. 4(e)], more commonly associated with "ice rules" in frustrated rare-earth antiferromagnets.[7]

In MnV_2O_4, the low-temperature canting transition has been associated with the ordering of V^{3+} orbital degrees of freedom,[17,24,25] and similar physics is likely at play here. Theoretically, it has been shown that the ground-state properties of both MnV_2O_4 (Ref. 24) and FeV_2O_4 (Ref. 35) are strongly influenced by the alternating pattern of trigonal distortion axes which now has been observed in both materials. The resultant physics is captured by the "quantum $120°$ model" analysis of Chern *et al.*,[25] who considered vanadium spinels with dominant trigonal distortions and showed for these materials that an orbitally ordered state is stabilized at low temperature with electron density modulated along $\langle 110 \rangle$

directions. The spin order is then determined by a competition between relativistic spin-orbit coupling and orbital exchange between vanadium sites. When the latter wins out, the ordered spins tend to lie along primary cubic axes in the plane perpendicular to the ordered A-site spins. When spin-orbit coupling is dominant, a strong single-ion anisotropy forces the spins to lie along cubic $\langle 111 \rangle$ directions and favors the two-in–two-out structure seen in Fig. 4. It has been shown that MnV_2O_4 is well described by an intermediate case, where spin-orbit coupling and orbital exchange are comparable.[25] The present data suggest that FeV_2O_4 is well within the strong spin-orbit coupling limit of this model. It is worth noting that strong spin-orbit coupling would have the additional effect of reducing the V^{3+} ordered moment size from spin-only values, consistent with observation.

From a pure physics perspective, the two-in–two-out spin structure itself may be one of the most interesting new observations. In the rare-earth pyrochlore antiferromagnets, a local two-in–two-out constraint arises from a net ferromagnetic coupling between Ising spins with a quantization axis along $\langle 111 \rangle$ and leads to the macroscopic ground-state degeneracy underlying the much-studied spin-ice class of compounds.[7] Our data imply that in FeV_2O_4 an equivalent Ising condition on vanadium spins results from the large trigonal distortion of the VO_6 octahedra in the presence of strong spin-orbit coupling. Thus, one way of interpreting the low-temperature magnetic state in this material is as a d-electron analog of the spin-ice problem, but persisting to temperatures as high as 60 K. In such a picture, the role of the large ordered spin on the Fe^{2+} site is to act as an applied field and break the macroscopic degeneracy; indeed, the magnetic order in the LTT phase is exactly what has been observed in spin-ice materials $Ho_2Ti_2O_7$ and $Dy_2Ti_2O_7$ with field applied along (001).[37] An analogous situation may be found in the "ordered spin-ice" phases of $Sm_2Mo_2O_7$[38] and $Nd_2Mo_2O_7$,[39] where rare-earth moments on the pyrochlore lattice couple to ferromagnetically ordered Mo spins. In $Tb_2Sn_2O_7$, a similar ordered spin-ice state has also been seen[40] and was initially associated with ferromagnetic near-neighbor coupling in the presence of moderate single-ion anisotropy. The results reported here provide an important link between such rare-earth pyrochlore antiferromagnets and trigonally distorted spinels such as FeV_2O_4.

*gmacdoug@illinois.edu

[1] P. G. Radaelli, New J. Phys. **7**, 53 (2004).

[2] S.-H. Lee *et al.*, J. Phys. Soc. Jpn. **79**, 011004 (2010).

[3] Q. Zhang, K. Singh, F. Guillou, C. Simon, Y. Breard, V. Caignaert, and V. Hardy, Phys. Rev. B **85**, 054405 (2012).

[4] D. B. Rogers, R. J. Arnott, A. Wold, and J. B. Goodenough, J. Phys. Chem. Solids **24**, 347 (1963).

[5] M. Tanaka, T. Tokoro, and Y. Aiyama, J. Phys. Soc. Jpn. **21**, 262 (1966).

[6]T. Katsufuji, T. Suzuki, H. Takei, M. Shingu, K. Kato, K. Osaka, M. Takata, H. Sagayama, and T.-h. Arima, J. Phys. Soc. Jpn. **77**, 053708 (2008).

[7]S. T. Bramwell and M. J. P. Gingras, Science **294**, 1495 (2001).

[8]Y. Ueda, N. Fujiwara, and H. Yasuoka, J. Phys. Soc. Jpn. **66**, 778 (1997).

[9]M. Reehuis, A. Krimmel, N. Büttgen, A. Loidl, and A. Prokofiev, Eur. Phys. J. B **35**, 311 (2003).

[10]S. H. Lee *et al.*, Phys. Rev. Lett. **93**, 156407 (2004).

[11]N. Nishiguchi and M. Onoda, J. Phys. Condens. Matter **14**, L551 (2002).

[12]R. Plumier and A. Tardieu, C. R. Hebd. Seances Acad. Sci. **257**, 3858 (1963).

[13]H. Mamiya, M. Onoda, T. Furubayashi, J. Tang, and I. Nakatani, J. Appl. Phys. **81**, 5289 (1997).

[14]E. Wheeler, B. Lake, A. T. M. N. Islam, M. Reehuis, P. Steffens, T. Guidi, and A. H. Hill, Phys. Rev. B **82**, 140406(R) (2010).

[15]K. Adachi, T. Suzuki, K. Kato, K. Osaka, M. Takata, and T. Katsufuji, Phys. Rev. Lett. **95**, 197202 (2005).

[16]T. Suzuki, M. Katsumura, K. Taniguchi, T. Arima, and T. Katsufuji, Phys. Rev. Lett. **98**, 127203 (2007).

[17]V. O. Garlea, R. Jin, D. Mandrus, B. Roessli, Q. Huang, M. Miller, A. J. Schultz, and S. E. Nagler, Phys. Rev. Lett. **100**, 066404 (2008).

[18]J. H. Chung, J.-H. Kim, S.-H. Lee, T. J. Sato, T. Suzuki, M. Katsumura, and T. Katsufuji, Phys. Rev. B **77**, 054412 (2008).

[19]H. Tsunetsugu and Y. Motome, Phys. Rev. B **68**, 060405(R) (2003).

[20]O. Tchernyshyov, Phys. Rev. Lett. **93**, 157206 (2004).

[21]N. B. Perkins and O. Sikora, Phys. Rev. B **76**, 214434 (2007).

[22]V. Pardo, S. Blanco-Canosa, F. Rivadulla, D. I. Khomskii, D. Baldomir, H. Wu, and J. Rivas, Phys. Rev. Lett. **101**, 256403 (2008).

[23]T. Maitra and R. Valenti, Phys. Rev. Lett. **99**, 126401 (2007).

[24]S. Sarkar, T. Maitra, R. Valenti, and T. Saha-Dasgupta, Phys. Rev. Lett. **102**, 216405 (2009).

[25]G. W. Chern, N. Perkins, and Z. Hao, Phys. Rev. B **81**, 125127 (2010).

[26]G. Shirane, D. E. Cox, and S. J. Pickart, J. Appl. Phys. **35**, 954 (1964).

[27]J. B. Goodenough, J. Phys. Chem. Solids **25**, 151 (1964).

[28]K. Tsuda, D. Morikawa, Y. Watanabe, S. Ohtani, and T. Arima, Phys. Rev. B **81**, 180102(R) (2010).

[29]S. Bordács, D. Varjas, I. Kézsmárki, G. Mihály, L. Baldassarre, A. Abouelsayed, C. A. Kuntscher, K. Ohgushi, and Y. Tokura, Phys. Rev. Lett. **103**, 077205 (2009).

[30]A. Krimmel, M. Mücksch, V. Tsurkan, M. M. Koza, H. Mutka, and A. Loidl, Phys. Rev. Lett. **94**, 237402 (2005).

[31]G. Chen, L. Balents, and A. P. Schnyder, Phys. Rev. Lett. **102**, 096406 (2009).

[32]S. Nishihara, W. Doi, H. Ishibashi, Y. Hosokoshi, X.-M. Ren, and S. Mori, J. Appl. Phys. **107**, 09A504 (2010).

[33]V. O. Garlea, B. C. Chakoumakos, S. A. Moore, G. B. Taylor, T. Chae, R. G. Maples, R. A. Riedel, G. W. Lynn, and D. L. Selby, Appl. Phys. A **99**, 531 (2010).

[34]See Supplemental Material at http://link.aps.org/supplemental/10.1103/PhysRevB.86.060414 for details regarding sample preparation and experimental methods, along with characterization data, full neutron powder diffraction patterns and refinement information. Also included is a discussion of the LTT-LTO structural and the spin-glass magnetic transitions, which were each suggested by previous experiments but are apparently absent in the current dataset.

[35]S. Sarkar and T. Saha-Dasgupta, Phys. Rev. B **84**, 235112 (2011).

[36]J.-S. Kang *et al.*, Phys. Rev. B **85**, 165136 (2012).

[37]T. Fennell, O. A. Petrenko, B. Fåk, J. S. Gardner, S. T. Bramwell, and B. Ouladdiaf, Phys. Rev. B **72**, 224411 (2005).

[38]S. Singh, R. Suryanarayanan, R. Tackett, G. Lawes, A. K. Sood, P. Berthet, and A. Revcolevschi, Phys. Rev. B **77**, 020406 (2008).

[39]Y. Taguchi, Y. Oohara, H. Yoshizawa, N. Nagaosa, and Y. Tokura, Science **291**, 2573 (2001).

[40]I. Mirebeau, A. Apetrei, J. Rodríguez-Carvajal, P. Bonville, A. Forget, D. Colson, V. Glazkov, J. P. Sanchez, O. Isnard, and E. Suard, Phys. Rev. Lett. **94**, 246402 (2005).